Microstructure and Magnetic Properties of Magnetron-Sputtered $[Fe/Pt]_n$ Multilayer Films

Y.M. Zhang[a,b], W.X. Yu[b], F.H. Chen[a], M. Liu[a] and H.B. Li[a,c,*]

[a]Key Laboratory of Functional Materials Physics and Chemistry of the Ministry of Education, Jilin Normal University, Siping 136000, PR China

[b]School of Materials Science and Engineering, Jilin University, Changchun 130025, PR China

[c]State Key Laboratory of Inorganic Synthesis and Preparative Chemistry, Jilin University, Changchun 130012, PR China

(Received September 9, 2014; in final form June 17, 2015)

$[Fe/Pt]_n$ multilayer films were prepared on thermally oxidized Si (100) substrates at 300 °C using dc magnetron sputtering and annealed for different temperature ranging from 350 to 500 °C. It is found that the as-deposited $[Fe/Pt]_n$ multilayer films exhibit well-resolved periodic structures and low roughness of interface. The ordering degree of the annealed films decreases and their perpendicular magnetic anisotropy deteriorates with increasing the period number. Fe/Pt bilayer film annealed at 350 °C shows (001) orientation and hard magnetic characteristic, the coercivity and perpendicular anisotropy enhance with increase of annealing temperature. In addition, the hard and soft magnetic phases are not fully magnetically coupled in the Fe/Pt film annealed at higher temperature.

DOI: 10.12693/APhysPolA.128.326

PACS: 68.55.Jk, 75.50.Ss

1. Introduction

To achieve higher magnetic recording density and signal-to-noise ratio simultaneously, the small grain size and weak intergranular exchange coupling are required [1]. $L1_0$ ordered FePt thin films are considered as one of the leading candidate materials for the next generation of the ultrahigh density magnetic recording media, because of their large uniaxial magnetic anisotropy, small superparamagnetic critical size, moderate saturation magnetization and excellent corrosion resistance [2]. Usually, FePt films deposited on amorphous or Si substrates tend to grow with (111) preferred or random orientations and its easy axis is tilted 37° away from the film plane. As the magnetic recording media, several efforts have been made toward high (001) orientation of $L1_0$ FePt film, such as epitaxial growth on a single crystalline substrate [3], buffer layer [4], and rapid thermal annealing [5], etc. But these methods result in the higher cost and annealing temperature. In general, the atomic arrangement of Fe and Pt in the $L1_0$ phase along the [001] direction is similar to atomic-scale Fe/Pt multilayer films [6, 7]. It has been demonstrated that the activation energy of $L1_0$ FePt formation from multilayer (≈0.7 eV) is lower than that of FePt formation from a homogeneous $A1$ phase (≈1.2 eV) [8]. The rapid interdiffusion of Fe and Pt at the interface is responsible for the formation of $L1_0$ FePt [9, 10]. The alternate deposition of Fe and Pt layer should be an effective method to obtain $L1_0$ FePt with (001) orientation. However, it is always a challenge to prepare high (001) orientation for the thinner film annealed at low temperature. Fe/Pt multilayer films deposited on heated substrate could solve the problem. The heated substrate is helpful in the interface diffusion between Fe and Pt layer and disorder-order phase transformation of the FePt film.

In this work, we reported the fabrication of $[Fe/Pt]_n$ multilayer films deposited on thermally oxidized Si (100) substrates at 300 °C. Each layer thickness of Fe and Pt was fixed at 2.5 nm. The as-deposited $[Fe/Pt]_n$ films were annealed at various temperatures. The structure, phase transformation and magnetic properties of the samples were investigated in detail.

2. Experiments

$[Fe\ (2.5\ nm)/Pt\ (2.5\ nm)]_n$ (n = 1, 4, 6, 8, 10) multilayer films (n is the period number) were prepared on thermally oxidized Si (100) substrates by dc magnetron sputtering on an ATC 1800-F magnetron sputtering system. The nominal temperature of the substrate was 300 °C. The purities of Fe and Pt targets were 99.99%. The base pressure of the deposition chamber was about 1.2×10^{-6} Torr, and Ar pressure was 5.0 mTorr during sputtering. The substrates were rotated at a speed of 20 rpm during deposition to obtain uniform films.

Film composition was measured using energy dispersive X-ray spectrometry (EDS) in Hitachi S-570 scanning electron microscope, the results were listed in Table. The as-deposited films were annealed at 350–500 °C in a vacuum furnace with a pressure about 3.0×10^{-6} Torr and the annealing time was fixed at 30 min. The structure of the as-deposited and annealed films were characterized by X-ray diffraction (XRD) on Rigaku D/max-2500

*corresponding author; e-mail: lihaibo@jlnu.edu.cn

diffractometer with Cu $K_{\alpha 1}$ radiation using a current of 300 mA and voltage of 40 kV. X-ray reflectivities (XRR) were measured on Philips X' Pert X-ray diffractometer with Cu K_{α} radiation using a current of 35 mA and voltage of 40 kV, with an attachment of the Göbel mirror. The magnetic properties of the films were measured at room temperature using Lake Shore 7407 vibrating sample magnetometer (VSM) with maximum applied field of 20 kOe.

TABLE

The composition of films measured using EDS.

Sample	Fe:Pt [at.%]
$n = 1$	50.5 : 49.5
$n = 4$	51.3 : 48.7
$n = 6$	51.0 : 49.0
$n = 8$	50.3 : 49.7
$n = 10$	51.0 : 49.0

3. Results and discussion

XRR curves of as-deposited $[Fe/Pt]_n$ (n = 1, 4, 6, 8, 10) films are shown in Fig. 1. For the $[Fe/Pt]_1$ film, the non-uniformity in the Kiessig fluctuations indicates that the film is composed of Fe and Pt bilayer structure. For the films with n = 4, 6, 8, 10, two or three Bragg peaks can be seen clearly due to the Fe/Pt multilayer structure. The appearance of the Bragg peaks provides the evidence that the $[Fe/Pt]_n$ films have a good periodic structure with composition modulation along the growth direction. The Kiessig fringe amplitude depends on the surface and interface roughness and the relative electron densities of the materials [11]. It is obviously noted that the multilayer films show low roughness of surface and interface on the basis of the distinct amplitude in the XRR curves of all the as-deposited films.

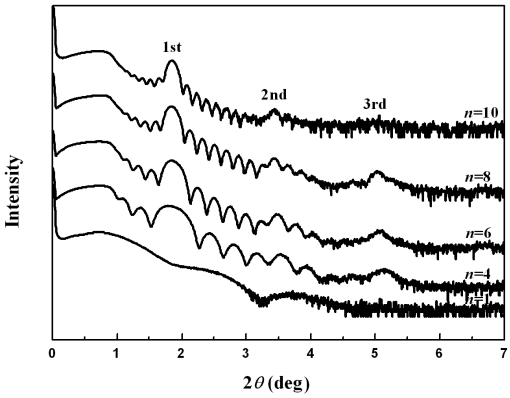

Fig. 1. XRR curves of the as-deposited $[Fe/Pt]_n$ films.

The modulation period Λ is defined as the sum of the thickness of one Fe and one Pt layer. Λ can be evaluated by the modified Bragg law [12]: $m\lambda/\sin\theta_m = 2\Lambda(1-\delta/\sin^2\theta_m)$, where θ_m is the angle position of reflection peaks in a low-angle X-ray diffraction spectrum, λ is the X-ray wavelength of 0.15406 nm, δ is related to the average refraction index of layer constituents by $n = 1-\delta$. Plotting $m\lambda/\sin\theta_m$ vs. $\sin^{-2}\theta_m$ produces a straight line with a slope of $-2\Lambda\delta$ and an interception of 2Λ on the $m\lambda/\sin\theta_m$ axis as shown in Fig. 2. Λ = 5.14, 5.25, 5.33 and 5.33 nm for the films with n = 4, 6, 8 and 10 are obtained, respectively. There is a good agreement between the modulation period obtained by using the modified Bragg law and the experimentally designed period. For the film with n = 1, the intensity of the reflection peak is too weak to calculate the modulation period.

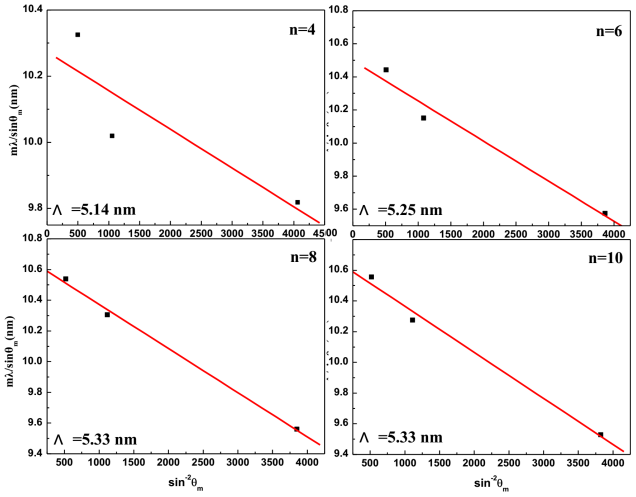

Fig. 2. Calculation of the modulation period using the modified Bragg law.

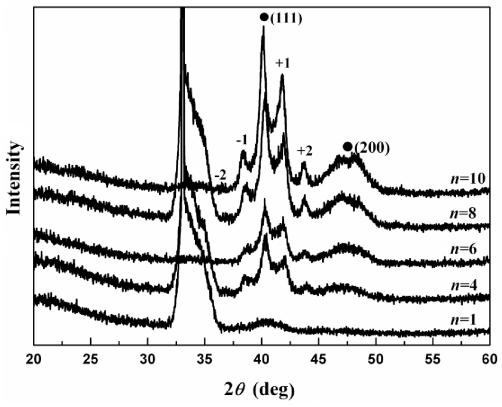

Fig. 3. XRD patterns of the as-deposited $[Fe/Pt]_n$ films.

XRD patterns of as-deposited $[Fe/Pt]_n$ films are shown in Fig. 3. The diffraction peaks around at $2\theta = 40.1°$ and 47.0° originate from the FePt (111) and (200) reflections of the face centered structure. For the $[Fe/Pt]_n$ films with n = 4, 6, 8 and 10, the first and second order satellite peaks (labelled −2, −1, +1 and +2, respectively)

located at both sides of the main diffraction peak are observed, which indicates that $[Fe/Pt]_n$ films have a superlattice structure. The intensity of satellite peaks increases with increasing n, which suggests that the film with larger n has a better and longer range structural coherence. The crystalline coherence length ξ along the growth direction can be estimated from the full width at half maximum (FWHM) of the main diffraction peak of the superlattice using the Scherrer formula [13]. For Fe/Pt superlattice films with $n = 4$, 6, 8 and 10, the crystalline coherence lengths ξ are 8.6, 7.6, 9.4, and 10.5 nm, respectively, which are greater than the modulation period. These results also reflect the good coherent growth between neighbouring Fe and Pt layers. When $n = 1$, only a broad and weak diffraction peak can be seen, which indicates that the film has very small grain size and weak crystallization.

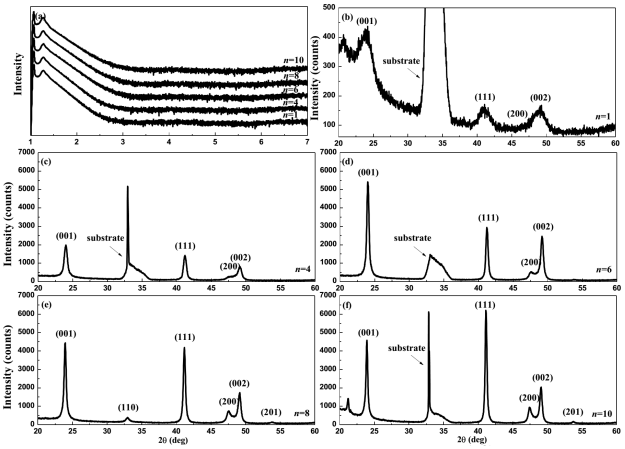

Fig. 4. (a) XRR curves and (b–f) XRD patterns of the $[Fe/Pt]_n$ films annealed at 400 °C.

Figure 4a illustrates XRR curves of $[Fe/Pt]_n$ films annealed at 400 °C. The XRR curves show the absence of the Kiessig fringes and the Bragg peaks, indicating that Fe/Pt multilayer structure disappears and interdiffusion between Fe and Pt layer occurs. $[Fe/Pt]_n$ films annealed at 400 °C are compositionally homogeneous. The variation of the XRR curves is in a good consistence with XRD results shown in Fig. 4b–f. In the XRD patterns of the films, the (001) superlattice, (110), (111), (200), (002), and (201) fundamental diffraction peaks of $L1_0$ ordered FePt phase emerge, indicating that the $L1_0$-FePt phase is formed. Hence, the interdiffusion at Fe/Pt interface occurs at 400 °C and the Fe/Pt multilayer structure transforms to compositionally homogeneous $L1_0$-FePt single layer structure.

To quantitatively describe the ordering degree of the FePt films, the ordering parameter S is introduced. An approximate relation between S and c/a (where c is the lattice constant along the chemical order direction and a is the lattice constant orthogonal to this) can be written as follows:

$$S^2 = \frac{1-(c/a)}{1-(c/a)_{S_f}},$$

where $(c/a)_{S_f} = 0.956$ is the axial ratio for the fully ordered phase [14], c/a is the axial ratio for the partially ordered phase and can be evaluated from the XRD patterns. In this equation, $S = 1$ corresponds to the fully ordered phase. Figure 5a shows the ordering degree S as a function of n. S can reach the maximum value of 0.94 when $n = 1$. It decreases with increasing n. It can be observed that the change in the degree of perpendicular orientation via the ratio of integrated intensity of (001) peak to that of the (111) peak of the FePt, is $I_{(001)}/I_{(111)}$, as shown in Fig. 5b. For the $L1_0$-FePt with a random distribution of easy magnetization axes, $I_{(001)}/I_{(111)} = 0.3$ (PDF#43-1359). In the case of $[Fe/Pt]_1$ film, $I_{(001)}/I_{(111)}$ can reach the maximum value of 2.8, which means that the $[Fe/Pt]_1$ film annealed at 400 °C has larger perpendicular magnetic anisotropy. The $I_{(001)}/I_{(111)}$ value decreases when n is larger than 1, indicating that the perpendicular magnetic anisotropy of the films deteriorates.

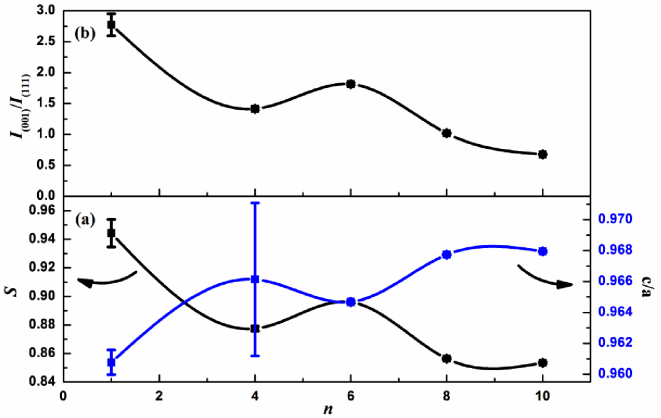

Fig. 5. Variations of (a) S and c/a, (b) $I_{(001)}/I_{(111)}$ for the films with period number n.

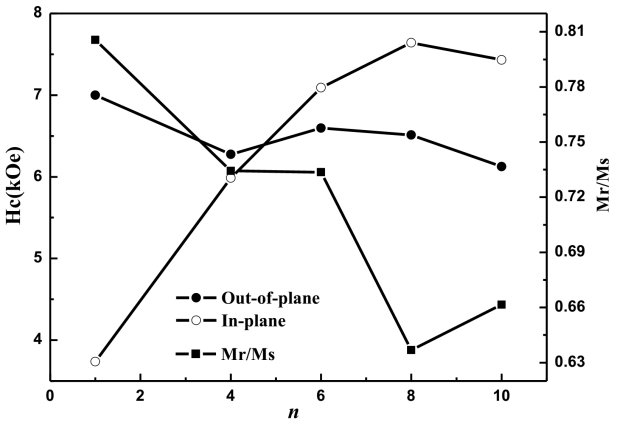

Fig. 6. Variations of out-of-plane and in-plane coercivities and out-of-plane remanence ratio M_r/M_s as a function of period number n for $[Fe/Pt]_n$ films.

Variations of out-of-plane ($H_{c_\perp}$) and in-plane coercivities ($H_{c_\parallel}$) and perpendicular remanence ratio M_r/M_s as functions of period number for $[\mathrm{Fe/Pt}]_n$ films are shown in Fig. 6. All films exhibit hard magnetic properties after annealing at 400 °C, which indicates that the $L1_0$ ordered structure is formed in the $[\mathrm{Fe/Pt}]_n$ films. For the film with $n = 1$, M_r/M_s can reach the maximum of 0.81, which indicates that the $[\mathrm{Fe/Pt}]_1$ film has the preferred alignment of the easy magnetization axis perpendicular to the film plane. This is consistent with the XRD results. $H_{c_\perp}$ and M_r/M_s decreases as n increases, $H_{c_\parallel}$ increases with n increasing, which suggests that the magnetic anisotropy of the FePt film changes gradually from perpendicular to random orientation. The change in the magnetic orientation might be caused by the sizes of FePt particle and magnetic domain. It has been reported that the average grain size and domain size increase with greater thickness of FePt film [15].

Figure 7 shows XRD patterns of the Fe/Pt ($n = 1$) bilayer films annealed at 350–500 °C. For the film annealed at 350 °C, a broad (111) diffraction peak of $L1_0$-FePt can be observed at around $2\theta = 41°$. When the annealing temperature is above 400 °C, (001) superlattice and (002) fundamental diffraction peaks of $L1_0$-FePt phase can be observed, suggesting that the films show (001) orientation. All of these peaks are broad, which indicates that the grain size of FePt is small. Kim et al. claimed that the size of the island-like grains depended on FePt film thickness strongly [16]. Kurth et al. also prepared the FePt (001) granular films with a nominal thickness in the range from 0.5 to 10 nm and examined the finite size effect [17]. Hence in order to decrease FePt particle size, it is necessary to control the film thickness.

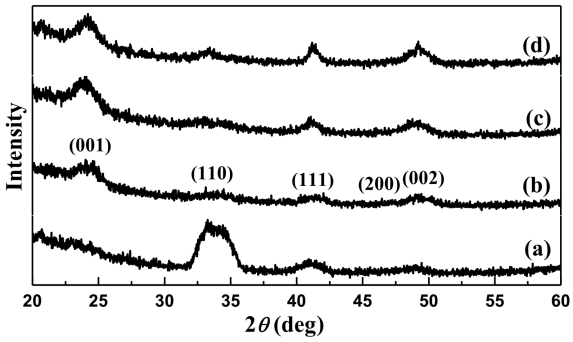

Fig. 7. XRD patterns of the Fe/Pt bilayer films annealed at (a) 350 °C, (b) 400 °C, (c) 450 °C and (d) 500 °C.

To further evaluate the degree of misorientation of the films annealed at different temperature, XRD rocking curves of (001) diffraction peaks were measured, and the results are shown in Fig. 8. It can be seen that the (001) half-peak widths of the annealed films decrease with increasing annealing temperature, which means that increase of the annealing temperature could improve the (001) orientation of $L1_0$ phase.

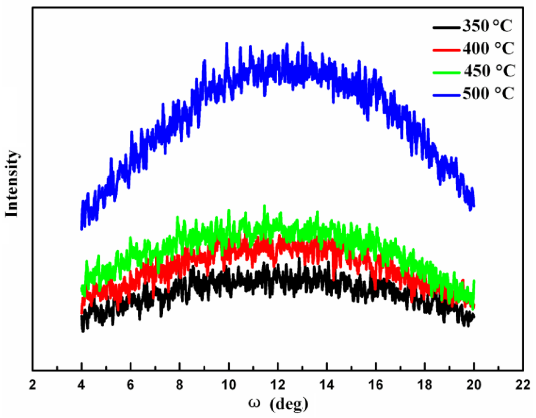

Fig. 8. XRD rocking curves of annealed Fe/Pt films.

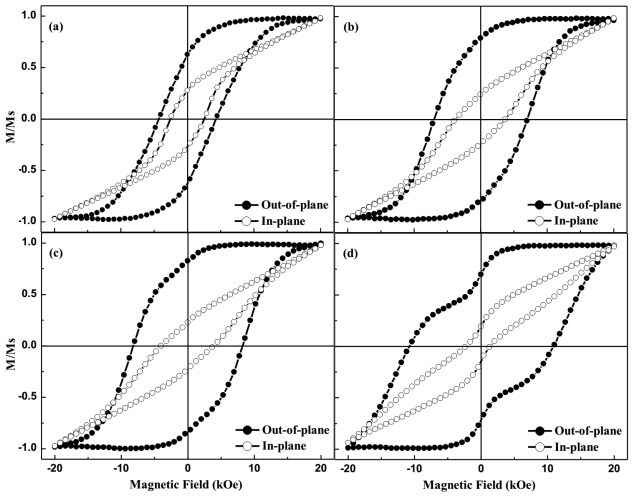

Fig. 9. Out-of-plane and in-plane hysteresis loops of the Fe/Pt bilayer films annealed at (a) 350 °C, (b) 400 °C, (c) 450 °C and (d) 500 °C.

The out-of-plane and in-plane hysteresis loops of Fe/Pt bilayer films annealed at 350–500 °C are represented in Fig. 9. For the Fe/Pt film annealed at 350 °C, the out-of-plane and in-plane coercivities are about 4.27 and 2.57 kOe, respectively. The hysteresis loops show the hard magnetic characteristic and the easy magnetization axis is in the out-of-plane direction due to (001) orientation of the film. When the annealing temperature is 400 °C, the contrast between out-of-plane loops and in-plane loops shows that the development of perpendicular anisotropy due to preferential (001) orientation. In the film with 450 °C annealing, the out-of-plane and in-plane coercivities have a further increase. As the annealing temperature increases to 500 °C, the out-of-plane and in-plane coercivities are about 10.88 and 1.82 kOe, respectively, suggesting that increasing annealing temperature could enhance the perpendicular anisotropy and hard magnetic properties of the films. Moreover, we can observe an apparent shoulder in the hysteresis loop, which indicates the presence of hard magnetic phase and soft magnetic phase that are not fully

magnetically coupled [18]. It has been reported that ordered phase was formed in a disordered grain via an inhomogeneous process [19], in which annealed FePt films contain ordered, partially ordered, and disordered regions. Accordingly, the high temperature processes cause normally grain growth, size dispersion, and intergranular coupling [20, 21]. Therefore, FePt film annealed at 500 °C will show magnetic multiphase properties due to increasing grain sizes. Also, the slope of the out-of-plane loop at coercivity $\alpha = 4\pi(\mathrm{d}M/\mathrm{d}H)_{H_c}$ [22] is the minimum value of 1.52 in the film annealed at 500 °C, indicating the weak exchange coupling between hard and soft magnetic phases.

4. Conclusions

The significant effect of the period number and annealing temperature on the structural and magnetic properties of $[Fe/Pt]_n$ films have been demonstrated. The as-deposited $[Fe/Pt]_n$ multilayer films have good periodic structure with composition modulation along the growth direction. The multilayer structure transforms to $L1_0$-FePt single layer structure after annealing at 400 °C, and the ordering and perpendicular magnetic anisotropy of the films deteriorates with increase of the period number. For the Fe/Pt film annealed at 350 °C, the out-of-plane and in-plane coercivities are about 4.27 and 2.57 kOe, respectively. When the annealing is carried out at higher temperatures, the perpendicular anisotropy and hard magnetic properties of the film are enhanced, while the hard and soft magnetic phases in the FePt film are not fully magnetically coupled due to larger grain sizes.

Acknowledgments

Project supported by National Natural Science Foundation of China (Grant No. 21371071).

References

[1] D. Weller, A. Moser, L. Folks, M.E. Best, W. Lee, M.F. Toney, M. Schwickert, J. Thiele, M.F. Doerner, *IEEE Trans. Magn.* **36**, 10 (2000).

[2] N. Kikuchi, S. Okamoto, O. Kitakami, *J. Appl. Phys.* **103**, 07D511 (2008).

[3] Z.H. Lu, J.B. Guo, Z.H. Gan, Y. Liu, R. Xiong, G.J. Mankey, *Appl. Phys. Lett.* **113**, 073912 (2013).

[4] I. Matsui, T. Ogi, F. Iskandar, K. Okuyama, *J. Appl. Phys.* **110**, 083906 (2011).

[5] S.N. Hsiao, S.H. Liu, S.K. Chen, F.T. Yuan, H.Y. Lee, *Appl. Phys. Lett.* **111**, 07A702 (2012).

[6] A. Martins, M.C.A. Fantini, N.M. Souza-Neto, A.Y. Ramos, A.D. Santos, *J. Magn. Magn. Mater.* **305**, 152 (2006).

[7] Y.H. Fang, P.C. Kuo, S.C. Chen, S.L. Hsu, G.P. Lin, *Thin Solid Films* **517**, 5185 (2009).

[8] Y. Endo, K. Oikawa, T. Miyazaki, O. Kitakami, Y. Shimada, *J. Appl. Phys.* **94**, 7222 (2003).

[9] B.M. Lairson, M.R. Visokay, R. Sinclair, B.M. Clemens, *Appl. Phys. Lett.* **62**, 639 (1993).

[10] Y. Ogata, Y. Imai, S. Nakagawa, *J. Appl. Phys.* **107**, 09A715 (2010).

[11] P. Colombi, D.K. Agnihotri, V.E. Asadchikov, E. Bontempi, D.K. Bowen, C.H. Chang, L.E. Depero, M. Farnworth, T. Fujimoto, A. Gibaud, M. Jergel, M. Krumrey, T.A. Lafford, A. Lamperti, T. Ma, R.J. Matyi, M. Meduna, S. Milita, K. Sakurai, L. Shabel'nikov, A. Ulyanenkov, A. Van der Lee, C. Wiemer, *J. Appl. Crystallogr.* **41**, 143 (2008).

[12] Q. Yang, L.R. Zhao, *Mater. Charact.* **59**, 1285 (2008).

[13] E.E. Fullerton, J.E. Mattson, S.R. Lee, C.H. Sowers, Y.Y. Huang, G. Felcher, S.D. Bader, *J. Appl. Phys.* **73**, 6335 (1993).

[14] S.C. Chen, T.H. Sun, *Vacuum* **84**, 1430 (2010).

[15] S.C. Chen, T.H. Sun, C.L. Chang, C.L. Shen, P.C. Kuo, J.R. Chen, *Thin Solid Films* **519**, 6964 (2011).

[16] C.S. Kim, J.J. Sapan, S. Moyerman, K. Lee, E.E. Fullerton, M.H. Kryder, *IEEE Trans. Magn.* **46**, 2282 (2010).

[17] F. Kurth, M. Weisheit, K. Leistner, T. Gemming, B. Holzapfel, L. Schultz, S. Fähler, *Phys. Rev. B* **82**, 184404 (2010).

[18] H.L. Su, S.L. Tang, N.J. Tang, R.L. Wang, M. Lu, Y.W. Du, *Nanotechnology* **16**, 2124 (2005).

[19] J.G. Na, *J. Mater. Sci. Lett.* **19**, 1171 (2000).

[20] N. Zotov, J. Feydt, A. Ludwig, *Thin Solid Films* **517**, 531 (2008).

[21] Z.R. Dai, Z.L. Wang, S.H. Sun, *Nano Lett.* **1**, 443 (2001).

[22] N. Honda, K. Ouchi, S. Iwasaki, *IEEE Trans. Magn.* **38**, 1615 (2002).